#3

ELECTROMAGNETIC WAVES IN PERIODIC STRUCTURES

LOUIS STARK

TECHNICAL REPORT NO. 208

DECEMBER 9, 1952

RESEARCH LABORATORY OF ELECTRONICS
MASSACHUSETTS INSTITUTE OF TECHNOLOGY
CAMBRIDGE, MASSACHUSETTS

The Research Laboratory of Electronics is an interdepartmental laboratory of the Department of Electrical Engineering and the Department of Physics.

The research reported in this document was made possible through support extended the Massachusetts Institute of Technology, Research Laboratory of Electronics, jointly by the Army Signal Corps, the Navy Department (Office of Naval Research), and the Air Force (Air Materiel Command), under Signal Corps Contract DA36-039 sc-100, Project 8-102B-0; Department of the Army Project 3-99-10-022.

MASSACHUSETTS INSTITUTE OF TECHNOLOGY

RESEARCH LABORATORY OF ELECTRONICS

Technical Report No. 208 December 9, 1952

ELECTROMAGNETIC WAVES IN PERIODIC STRUCTURES

Louis Stark

This report is based on a thesis submitted to the Department of Electrical Engineering, M.I.T., in partial fulfillment of the requirements for the degree of Master of Science, May 1952.

Abstract

A few of the properties of electromagnetic waves in periodic structures are considered, with some discussion of propagation in open-boundary structures. Iris-loaded waveguides of standard cross section are then analyzed to obtain an accurate solution for the propagation constant. A measurement performed on a loaded rectangular waveguide shows the calculation to be quite accurate. An experimental and analytical investigation of the so-called interleaved-fin structure to judge its application as a slow-wave circuit for traveling wave amplifiers is described.

ELECTROMAGNETIC WAVES IN PERIODIC STRUCTURES

I. Introduction

The theory of electromagnetic fields in periodic structures has important applications in the field of microwave electronics, and it is this aspect of the subject that has supplied the motivation for much of the investigation described in this report. It is probably impossible to analyze rigorously the electronic devices using these structures, but one approximate approach, which is good when the free electron current density is small, is to make use of the fields in the charge-free structure. This technique is applicable in the case of the linear accelerator tube and, through J. R. Pierce's simplified theory of traveling wave amplification (8), to the small-beam-current traveling wave tube. In certain cases another approach, not having the small current density limitation, is possible. This is a direct solution of the problem (current density present), in which an initial simplifying approximation is made by substituting appropriate smooth boundaries for the periodic boundaries (see, for example, ref. 9). Our interest here, however, arises from the first approach; we are concerned, in particular, with the following properties of the structure fields: (a) the phase velocities of the space harmonic components of the field, (b) the axial electric field strength of these wave components. After a brief statement of a few simple properties of fields in periodic structures, two specific problems will be considered.

The first of these problems deals with an accurate solution for the propagation constant in iris-loaded waveguides of standard cross section. In more or less specialized forms, this problem has been treated extensively in the literature. (Consult refs. 1 through 5.) A segmented treatment of this problem is in certain respects desirable, since the approach that leads to the most simple and accurate numerical solution depends to some extent upon the range in which the variables (frequency and the parameters of the geometry) fall. Nevertheless, in section III an attempt is made at unifying the problem by presenting a result which is common to all the standard types of waveguide cross sections and is general to the extent that the loading irises can be taken to be infinitely thin. The formal result is expressed as a quotient of infinite sums whose terms depend upon the field distribution in the aperture (which is always a complete standing wave). The result can be solved to a quasi-stationary approximation, and in the case of the rectangular guide, it is possible to virtually sum the series so that the result is useful in practice. Calculated and measured results for a particular guide are compared in Fig. 4.

The second major problem with which we shall be concerned is somewhat more specific than the first. It is the investigation of the use of the so-called interleaved-fin structure as a slow-wave circuit for traveling wave amplifiers. Proceeding from Pierce's simplified theory of traveling wave amplification, we use a combined experimental and analytical approach to determine the pertinent properties of the circuit fields.

The structure is considered for the case of either open or closed lateral boundaries parallel to the y, z plane (see Fig. 6); it is found that certain advantages accrue in each case. Though the geometry of the structure makes an exact field-theory analysis impossible, there is an approximate way of treating the structure, which is shown by experiment to be quite accurate. Basically, we look at the structure as a folded rectangular waveguide having either open-circuited or short-circuited side walls. The basis for substituting open-circuited (magnetic) walls for the open lateral boundaries rests on experimental observations, and we find that this approximation is quite good, provided the axial propagation constant does not lie in or close to certain "forbidden regions," which will be discussed later. The discontinuity at each bend of the folded guide is accounted for by an equivalent network whose parameters are calculated at some length in Appendix B. Although most of the theory neglects the presence of the beam transmission holes, experiment shows that the propagation constant is only negligibly affected by the introduction of even relatively large holes. The degree to which the circuit will couple to a given beam, measured by Pierce's impedance definition, is difficult to determine experimentally and is calculated from the field distribution in the model. In general, the structure can support a relatively high impedance space harmonic that can be made to travel either with or against the flow of power. Though the phase velocity of the high-impedance wave will be found to vary with the frequency, reasonably large amplifying bandwidths are possible with medium-to-high perveance, high-voltage electron beams.

Before proceeding to the details of the two special problems, we shall obtain in the following section some general results which will be of help in these discussions.

II. Some Basic Properties of the Modes

2.1 Introduction

In this section we will be concerned with some of the fundamental properties of waves in periodic structures. The discussion that follows is not intended to be a comprehensive treatment of the subject, but is directed at a few special ideas that will serve as a background for experimental and analytical work on some particular structures in sections III and IV. The interest will be in the free modes of propagation in these structures, that is, those which persist at indefinitely large distances from a source. The general type of structure considered may have lateral boundaries which are closed by conducting walls, or open to the outside world. A periodicity L is assumed along the propagation axis (taken to be the z-axis), although periodicity in other directions is not excluded. The field quantities are assumed to vary harmonically with time, and the factor $\exp(j\omega t)$ is understood.

2.2 Floquet's Theorem and the traveling wave definition

The wave solutions for periodic structures are distinguished from those for the uniform waveguide in that in the former case the field distribution is not the same in every transverse plane. The modes of oscillation in periodic structures are described by Floquet's Theorem,* which states that in a given mode and at a given frequency, the electromagnetic fields at any pair of corresponding points separated by a period L are related by the same constant factor. Traveling waves are defined by choosing a complex number as the constant factor in order to impart a phase shift between the fields at points separated by a period. In the case of a single traveling wave, if the medium is lossless and no energy is lost by radiation (should the structure have open boundaries), the complex number must have magnitude unity. Let the constant factor then be written $\exp(-jh_oL)$ to give a phase shift of h_oL radians over a period. One need not go any further in formulating traveling waves in periodic structures; however, in some types of analyses it is convenient to introduce the space harmonic concept, which is deduced as follows. The most general type of z-dependence which multiplies the fields by $\exp(-jh_oL)$ as we move down the structure a period is the function $\exp(-jh_oz)$ times a function of z of periodicity L. If the periodic function is written in complex Fourier series form and multiplied by $\exp(-jh_oz)$, the field quantities can be written as a sum of space harmonics

$$F = \sum_{n=-\infty}^{\infty} f_n \exp\left[-j\left(h_o + \frac{2\pi n}{L}\right) z\right] \tag{1}$$

where f_n expresses the transverse dependence of the n-th space harmonic of the vector field component F. In this light, h_o is the fundamental propagation constant or the propagation constant of the zeroth space harmonic.

2.3 Relation between stored energy, power flow, and group velocity

In the well-known theory of uniform waveguides a relation is established between time average, axial power flow P, stored energy per unit length W, and frequency rate of change of the propagation constant h, namely

$$P = \frac{W}{dh/d\omega} \tag{2}$$

$1/(dh/d\omega)$ can be interpreted physically as the velocity of energy propagation and is given the name, group velocity. Equation 2 is useful in establishing certain proofs. Many authors have used it directly, substituting h_o for h, in the analysis of periodic structures. One readily observes, however, that Eq. 2, as it stands, is meaningless for periodic

*A good part of the discussion on Floquet's Theorem is drawn from reference (1), p. 6.

structures, since the energy stored per unit length is generally a function of position along the propagation axis, whereas the axial power flow is not. In terms of the energy stored in any one period of the structure W_L one might expect a relation of the form

$$P = \frac{W_L/L}{dh_o/d\omega} \tag{3}$$

to exist. This in fact proves to be the case.

The proof of Eq. 3 comes from the energy theorem (see ref. 6, p. 55)

$$\nabla \cdot \left[\bar{E}^* \times \frac{\partial \bar{H}}{\partial \omega} + \frac{\partial \bar{E}}{\partial \omega} \times \bar{H}^*\right] = -j\left[\epsilon \bar{E} \cdot \bar{E}^* + \mu \bar{H} \cdot \bar{H}^*\right] \tag{4}$$

which is obtained by frequency differentiation of the Maxwell equations. Here, $\bar{E}$ and $\bar{H}$ are complex field vectors which are functions of all space coordinates. The procedure will be to integrate Eq. 4 over a volume bounded laterally by a cylindrical surface and on the ends by transverse planes separated by a period of the structure. If the structure is closed by conducting walls, then the lateral surface is taken to lie on the walls, whereas if the structure has open boundaries, the surface is chosen to lie at infinity. Integrating the right side of Eq. 4 over such a volume yields simply $-4jW_L$. To integrate the left side, use is made of the divergence theorem, which gives

$$\int_V \nabla \cdot \left[\bar{E}^* \times \frac{\partial \bar{H}}{\partial \omega} + \frac{\partial \bar{E}}{\partial \omega} \times \bar{H}^*\right] dV = \oint_S \left[\bar{E}^* \times \frac{\partial \bar{H}}{\partial \omega} + \frac{\partial \bar{E}}{\partial \omega} \times \bar{H}^*\right] \cdot \bar{n}\, dS \tag{5}$$

where $\bar{n}$ is the outward normal to the closed surface S bounding V. The contribution due to integration over the lateral surface is zero in the case of conducting walls since $\bar{n} \times \bar{E}$ is zero on the walls; it is zero in the case of open boundaries since the fields must vanish faster than $(1/r^{1/2})$ at large distances. (This restriction is necessary to insure that the structure is not radiative (see subsec. 2.4).) Choosing the propagation axis to be the z-axis and denoting the field quantities in the plane $z = z_1$ by subscript 1 and those in the plane $z = z_1 + L$ by subscript 2, we have

$$\int_{T\ \text{plane}} \bar{i}_z \cdot \left[-\left(\bar{E}_1^* \times \frac{\partial \bar{H}_1}{\partial \omega} + \frac{\partial \bar{E}_1}{\partial \omega} \times \bar{H}_1^*\right) + \left(\bar{E}_2^* \times \frac{\partial \bar{H}_2}{\partial \omega} + \frac{\partial \bar{E}_2}{\partial \omega} \times \bar{H}_2^*\right)\right] dS = -4jW_L \tag{6}$$

Since the fields in planes separated by a period are related by the factor $\exp(-jh_oL)$, we have

$$\bar{E}_2 = \bar{E}_1 \exp(-jh_oL), \quad \bar{H}_2 = \bar{H}_1 \exp(-jh_oL)$$

$$\bar{E}_2^* = \bar{E}_1^* \exp(jh_oL), \quad \bar{H}_2^* = \bar{H}_1^* \exp(jh_oL)$$

Performing the frequency derivatives and canceling terms, we find

$$-jL\frac{dh_o}{d\omega}\int_T \bar{i}_z \cdot \left(\bar{E}_1^* \times \bar{H}_1 + \bar{E}_1 \times \bar{H}_1^*\right) dS =$$

$$-4jL\frac{dh_o}{d\omega}\int_T \bar{i}_z \cdot \left[\frac{1}{2}\,\mathrm{Re}\left(\bar{E}_1 \times \bar{H}_1^*\right)\right] dS = -4jW_L \tag{7}$$

which, in view of the complex Poynting Theorem, can be written

$$P_{+z} = \frac{W_L/L}{dh_o/d\omega} \tag{8}$$

This is the relation which was to be proved. There is an important result of this relation which will be useful later. Since W_L is a nonnegative quantity, P_{+z} and $(dh_o/d\omega)$ must always be of the same sign. If we always take the source to be at $z = -\infty$, then P_{+z} is nonnegative and $(dh_o/d\omega)$ must always be positive or zero. Nothing in the derivation prohibits h_o from being negative. This allows for the situation in which phase and "group" velocities are of opposite sign.

2.4 Forbidden regions of the propagation constant for open-boundary structures

S. Sensiper, in his solution for the free modes of propagation on a wire helix (7), discovered that there are periodic ranges of disallowed values of the propagation constant for this structure. Using an elementary approach, we shall show that this phenomenon is true for any open-boundary structure having periodicity along the propagation axis.

If the structure is to support a free mode, there can be no power loss in the propagating wave. If it is found that the propagation constant of the assumed free mode is such that power leaves the structure by radiation, then the assumption of a free mode having the given propagation constant is contradicted. Such values of the propagation constant are called (after Sensiper) "disallowed values," and when plotted in a certain plane, they fall in the "forbidden regions." In seeking the radiation condition, we are led to consider the open-boundary periodic structure as an infinitely extending antenna array.

Now suppose that the structure is propagating a free mode. Focusing attention on one period, we can in principle calculate the far-field pattern due to the current distribution on this period. Adopting the coordinate system shown in Fig. 1, let the pattern in an arbitrary plane through the z-axis be some function of ϕ, say $F(\phi)$. From straightforward linear antenna-array analysis (see ref. 10, p. 342) it follows that the pattern due to n periods separated a distance L with a phase shift $h_o L$ between is

$$\frac{F_n(\phi)}{F(\phi)} = \frac{\sin\frac{n}{2}(kL\cos\phi - h_o L)}{\sin\frac{1}{2}(kL\cos\phi - h_o L)}, \quad k = \frac{\omega}{c} \tag{9}$$

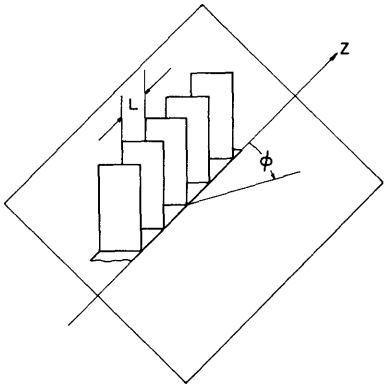

Fig. 1

The coordinate ϕ in an arbitrary plane through the z-axis.

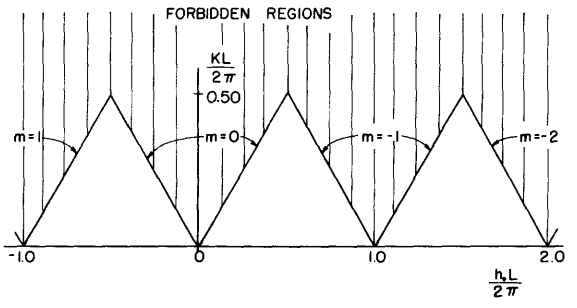

Fig. 2

Map of the forbidden regions of the propagation constant for open-boundary structures.

As we consider the result of adding the effects of an increasingly greater number of periods ($n \to \infty$), the over-all pattern approaches a series of infinities, located at values of ϕ such that

$$\frac{1}{2}(kL \cos \phi - h_o L) = m\pi, \quad m = 0, \pm 1, \pm 2, \ldots \tag{10a}$$

or at

$$\phi = \pm \cos^{-1}\left(\frac{h_o L + 2m\pi}{kL}\right), \quad m = 0, \pm 1, \pm 2, \ldots \tag{10b}$$

If no power is to leave the structure by radiation, the infinities must not occur at any real values of ϕ. Thus, we conclude that allowed values of the propagation constant must satisfy the inequality

$$|h_o L + 2m\pi| > kL$$

or

$$\left|\frac{h_o L}{2\pi} + m\right| > \frac{kL}{2\pi}, \quad m = 0, \pm 1, \pm 2, \ldots \tag{11}$$

When the inequality (Eq. 11) becomes an equality, the forbidden-region boundaries are defined. These plot in the $(kL/2\pi,\ h_o L/2\pi)$ plane as in Fig. 2. If the mode is resolved into a set of space harmonics (see Eq. 1), it is seen that free-mode propagation can occur only if each space harmonic has a phase velocity less than that of homogeneous plane waves in the medium.

It is worth while to determine the form of the radial dependence of the fields at large distances normal to the propagation axis. For this purpose we can enclose the structure by an imaginary cylindrical surface and express the fields outside in terms

of the wave functions of the circular cylinder. Outside the surface, as inside, the z-dependence of the fields must be given by a sum of exponential dependences, representing the space harmonics of the field. The form of the n-th space harmonic component, having the propagation constant, $h_n = h_o + (2\pi n/L)$, is

$$F_n = \exp(-jh_n z) \sum_m K_m \left[\left(h_n^2 - k^2 \right)^{1/2} r \right] \begin{cases} a_m \cos m\theta \\ b_m \sin m\theta \end{cases} \tag{12}$$

Now, for large values of the argument, the K_m functions approach the same value for all m; this value is proportional to

$$(1/r^{1/2}) \exp\left\{ -\left[\left(h_n^2 - k^2 \right)^{1/2} r \right] \right\}$$

Thus, at large radius, the radial dependence of the n-th space harmonic component is

$$F_n(r) \sim \frac{\exp\left\{ -\left[\left(h_n^2 - k^2 \right)^{1/2} r \right] \right\}}{r^{1/2}} \tag{13}$$

The radial dependence of the total field is generated by a sum over n of the terms (Eq. 13); hence, the total field is a rapidly decaying (though, not necessarily monotonic) function of radius. This being the case, one would not expect the field distribution of a free mode to be significantly altered by the introduction of a closed conducting shield having a relatively large radius.

When any of the space harmonic components has a wavelength greater than the free-space wavelength, k^2 is greater than h_n^2 (for some n) and the argument of the exponential function in Eq. 13 becomes imaginary. This form of radial dependence represents an outward traveling wave, which dies off in magnitude only as $(1/r^{1/2})$. When this is the case, one will not find a free mode propagating unless the shield is present to insure that the radiation condition is not violated. Here, the conducting shield becomes a very important part of the waveguide, and we find that a large fraction of the total field energy is stored in the space between the structure and the shield.

In practice, structures used with traveling-wave tubes of the beam type are almost always shielded by the shell of a beam-focusing electromagnet. In this case, a radiation condition is not possible, and there are no forbidden regions of the propagation constant. However, it is still well to keep these regions of the propagation constant in mind since they serve to indicate a radical change in the field structure and possibly a greatly reduced coupling between the circuit and beam. As long as each space harmonic

has a phase velocity less than that of light, it will be a good approximation to neglect the presence of the shell in determining the fields.

2.5 Periodic structures as resonators

Under the proper conditions, a standing wave on a periodic structure can be confined between perfectly conducting transverse planes. If the structure has closed lateral boundaries, then the planes close the ends of the structure to form a cavity. If the structure is open, then the planes must in principle extend indefinitely in the transverse direction. We will formulate the conditions for the existence of fields in the resonator in the manner in which these problems are usually handled, that is, by considering the total field to be constructed from a pair of free modes propagating in opposite directions. If a transverse plane can be located along the propagation axis at a position such that the structure has even symmetry about the plane, then waves incident upon the plane from opposite directions can be phased so that there is complete cancellation of the transverse electric fields in the plane. The fields in each traveling wave are multiplied by $\exp\left[\pm j(mh_oL)\right]$ as we move m structure periods away from this node; hence, if $mh_oL = q\pi$ (q is any integer), we are at another node. Conducting planes can be inserted at each of the nodes to confine the standing wave, and the boundary conditions are automatically satisfied. The existence of fields in the resonator is thus possible if the end planes are separated by an integer number of structure periods and each plane is so disposed that the structure has even symmetry about the plane. (The proper disposition of one plane, of course, automatically insures the proper disposition of the other when the planes are separated by a whole number of periods.) If these geometrical conditions are satisfied, resonances will occur only when

$$\frac{h_oL}{\pi} = \frac{q}{m}$$

where q = 1, 2, 3, . . ., and m = the number of periods between planes. If these geometrical conditions are not satisfied, resonances will generally occur, but they will not be related in any simple way to the propagation constant of a free mode.

If the symmetry requirement can be satisfied for one location of a plane, it can also be satisfied at another location which is one half a structure period removed from the first. Unless the structure is self-resonant, the preceding development is valid for either location. When the structure is self-resonant, the device of using oppositely directed traveling waves with controllable phase is not valid, and here the method fails. In this case, if the structure periods have even symmetry about a plane, there will be short-circuit planes (whose positions are easily deduced) at which conducting surfaces can be placed to confine the standing wave.

III. The Propagation Characteristic for Iris-Loaded Waveguides of Standard Cross Section

3.1 Introduction

A number of basically different types of periodic structures can provide for the transmission of a "slow wave" with strong axial electric field. If it is not required that the wave velocity be relatively independent of the frequency, the physically simple iris-loaded waveguide can be used to support the wave. This structure has been considered for practical application with the linear accelerator tube and for use as a slow-wave circuit for traveling wave amplifiers (1, 2, 3, 4, 5, 8). Outside the field of microwave electronics, the loaded waveguide has been used as a foreshortened delay line for phasing antenna arrays. As a special type of microwave circuit, a short-circuited length of the loaded guide can be used as a cavity resonator. Each use for the loaded guide places specialized requirements on performance; in section IV some of the requirements pertinent to traveling wave amplification will be noted. Of primary interest in all applications is an accurate determination of the propagation constant h_o.

J. C. Slater has given an accurate solution for the π-mode frequencies for loaded, round waveguides (2). The technique used is equally applicable to waveguides with other standard cross sections. A solution for the traveling wave problem, obtained by W. Walkinshaw (3), is very accurate as long as the phase shift over a period of the structure is not too large. In reference 3, excellent experimental agreement with Walkinshaw's calculation is shown for $h_o L \leqslant (2/7)\pi$. For applications to traveling wave linear accelerators and traveling wave amplifiers, the case of a small phase shift over a period is often useful since it results in a dominant space harmonic. For some applications, however, it might be useful to have a means of accurately predicting the propagation constant over the entire range of the first passband, $0 \leqslant h_o L \leqslant \pi$. In this section we will develop a method of carrying out this calculation for the case of infinitesimally thin irises in the commonly occurring waveguide cross sections. Using characteristic function expansions, we first obtain the exact solution to the problem. It is impossible to use this solution in practice, but we find that it indicates an approximate method of solution which should be quite accurate if the iris hole is not too large a fraction of the free-space wavelength.

Numerical computations, though generally somewhat tedious, are carried out most readily for those problems in which the iris spacing is comparable with the transverse extent of the waveguide.

3.2 Formal solution for the propagation constant

Three types of waveguide of practical importance are those with rectangular, circular, and concentric circular cross sections. We shall be concerned with the case of periodic loading by capacitive irises symmetrically located in the cross section of these guides.

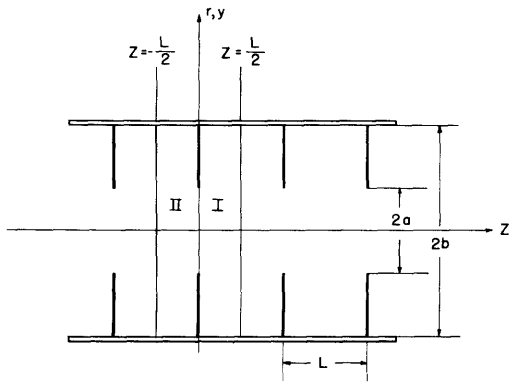

Fig. 3
The iris-loaded waveguide.

In the case of guides with circular symmetry, only fields with no angular variation are considered. The problem of a rectangular waveguide with capacitive irises is most simply solved by first solving the corresponding problem in an infinite parallel plane waveguide and then making a simple substitution for the wave number. In all these cases, the fields will be a sum of E waves and (possibly) a TEM wave, which vary with one transverse coordinate only. In the development which follows, it proves simplest to deal with the general E wave functions in the initial part of the calculation; at a later stage, the problem is specialized to a given geometry by substituting the appropriate set of characteristic functions.

Let the coordinate system be chosen as in Fig. 3. Here, we have indicated a longitudinal section of the rectangular or circular guide; obvious additional lines will include the case of a concentric line waveguide. Because of the periodic nature of the field distribution, we need consider the fields in only one period of the structure. Let the period be bounded by the planes $z = \pm(L/2)$. Further, let this period be divided into two regions, the interface lying in the plane of the iris, $z = 0$. In each region the uniform waveguide equations are valid; the complete set of waveguide modes will represent the most general type of field distribution that can exist in each region. A unique solution is obtained from the general solutions in each region by (a) matching the total transverse electric and magnetic fields across the interface, and (b) using the periodicity condition to relate the fields at $z = +(L/2)$ to those at $z = -(L/2)$. Thus, we write for the fields in region I

$$\bar{E}_{T1} = \sum_n \nabla_T \phi_n (A_n \cosh k_n z + B_n \sinh k_n z) \tag{14a}$$

$$\bar{H}_{T1} = \sum_n \frac{jk\eta}{k_n} \nabla_T \phi_n \times \bar{i}_z (A_n \sinh k_n z + B_n \cosh k_n z) \tag{14b}$$

$$E_{z1} = \sum_n \frac{p_n^2 \phi_n}{k_n} (A_n \sinh k_n z + B_n \cosh k_n z) \tag{14c}$$

where

$$k = \frac{\omega}{c}, \quad k_n^2 = p_n^2 - k^2; \quad \nabla_T = \nabla - \bar{i}_z \frac{\partial}{\partial z}; \quad \eta = \left(\frac{\epsilon}{\mu}\right)^{1/2}$$

and ϕ_n is a solution of $\left(\nabla_T^2 + p_n^2\right)\phi_n = 0$, subject to the boundary condition on the waveguide wall

$$\phi_n = 0, \quad p_n \neq 0 \quad \text{(E wave)}$$

$$\bar{n} \times \nabla_T \phi_n = 0, \quad p_n = 0 \quad \text{(TEM wave)}$$

where $\bar{n}$ is a vector normal to the waveguide wall. The wave functions in region II differ from those in region I only by amplitude factors. Thus, in region II

$$\bar{E}_{T2} = \sum_n \nabla_T \phi_n (C_n \cosh k_n z + D_n \sinh k_n z) \tag{15a}$$

$$\bar{H}_{T2} = \sum_n \frac{jk\eta}{k_n} \nabla_T \phi_n \times \bar{i}_z (C_n \sinh k_n z + D_n \cosh k_n z) \tag{15b}$$

$$\bar{E}_{z2} = \sum_n \frac{p_n^2 \phi_n}{k_n} (C_n \sinh k_n z + D_n \cosh k_n z) \tag{15c}$$

with the same definitions as before.

Now, at $z = 0$, transverse electric field is continuous across the entire waveguide cross section. Because of the orthogonality of the $\nabla_T \phi_n$ over this region, we must have

$$A_n = C_n, \quad n = 0, 1, 2, \ldots \tag{16}$$

Further, at $z = 0$, transverse magnetic field is continuous over the aperture region. Thus, subtracting $\bar{H}_{T2}$ from $\bar{H}_{T1}$ at $z = 0$,

$$\sum_n \nabla_T \phi_n \times \bar{i}_z \frac{B_n - D_n}{k_n} = 0 \tag{17}$$

over the aperture. There remains the relation between the field quantities in planes separated by a period

$$\bar{E}_{T1}\left(\frac{L}{2}\right) = \bar{E}_{T2}\left(\frac{-L}{2}\right) \exp(-jh_o L) \tag{18a}$$

$$\bar{H}_{T1}\left(\frac{L}{2}\right) = \bar{H}_{T2}\left(\frac{-L}{2}\right) \exp(-jh_o L) \tag{18b}$$

Because of the orthogonality of the transverse parts of the wave functions over the guide cross section, this relation must hold for each of the transverse parts separately. Thus, from Eqs. 14a, 15a, 14b, and 15b, the amplitude factors in the wave functions must satisfy the relation

$$A_n \cosh \frac{k_n L}{2} + B_n \sinh \frac{k_n L}{2} = \exp(-jh_o L) \left(C_n \cosh \frac{k_n L}{2} - D_n \sinh \frac{k_n L}{2}\right) \tag{19a}$$

$$A_n \sinh \frac{k_n L}{2} + B_n \cosh \frac{k_n L}{2} = \exp(-jh_o L) \left(D_n \cosh \frac{k_n L}{2} - C_n \sinh \frac{k_n L}{2}\right) \tag{19b}$$

where n = 0, 1, 2, ... Solving these equations for $(B_n - D_n)$, using Eq. 16, and substituting in Eq. 17, we find

$$\sum_n \frac{A_n}{k_n}\left(\tanh\frac{k_nL}{2}\cos^2\frac{h_oL}{2} + \coth\frac{k_nL}{2}\sin^2\frac{h_oL}{2}\right)\nabla_T\phi_n \times \bar{i}_z = 0 \qquad (20)$$

over the aperture.

Equation 20 is the end result of satisfying all the physical requirements of the problem; it expresses the fact that at a given frequency, the amplitudes A_n and the propagation constant h_o must be such that the function given by the left side of Eq. 20 vanishes at every point of the aperture. The vanishing of the function is insured by having all of its Fourier components vanish; that is, we satisfy the requirement by setting equal to zero the integrated scalar product of the left side of Eq. 20 and each member of a complete set of functions which are orthogonal over the aperture domain. Thus, denoting members of the orthogonal set by

$$\nabla_T\psi_m \times \bar{i}_z, \quad m = 0, 1, 2, \ldots \qquad (21)$$

we can write

$$\sum_n \frac{A_n}{k_n}\left(\tanh\frac{k_nL}{2}\cos^2\frac{h_oL}{2} + \coth\frac{k_nL}{2}\sin^2\frac{h_oL}{2}\right)I_{mn} = 0, \qquad m = 0, 1, 2, \ldots \qquad (22)$$

where

$$I_{mn} = \int_A (\nabla_T\phi_n \times \bar{i}_z)\cdot(\nabla_T\psi_m \times \bar{i}_z)\,dS = \int_A (\nabla_T\phi_n \cdot \nabla_T\psi_m)\,dS \qquad (23)$$

A particular waveguide geometry determines the functions $\nabla_T\phi_n$, and a convenient choice for the functions of Eq. 21 determines the coefficients I_{mn}. In this form one sees that Eq. 22 constitutes the exact solution of the problem for these equations have nontrivial solutions for the A_n only if the determinant of the coefficients vanishes. The determinantal equation furnishes the solution for h_o, and from Eqs. 16, 19a, and 19b, we can calculate the remaining wave amplitudes. Because of the infinite extent of the determinant, this procedure cannot be carried out in practice. The exact formal solution is useful, however, in that it leads to a method of operating on Eq. 20 which should be quite accurate in determining the propagation constant approximately. One notes that the functions $\nabla_T\phi_n$ and $\nabla_T\psi_m$ can be chosen, without loss in generality, to be pure real functions. Thus the coefficients of A_n in Eq. 22 are all real, and a proof in the theory of determinants (ref. 15, p. 25) states that the A_n must all be real or, at most, all

real numbers multiplied by the same complex constant. From Eq. 14a one sees that the A_n are the Fourier coefficients for the expansion of transverse electric field at $z = 0$ in the functions $\nabla_T \phi_n$. Thus, as we might have guessed from physical reasoning, the transverse electric field in the aperture is a complete standing wave. This being the case, it is not difficult to fit a good quasi-static approximation to the aperture field and determine the coefficients A_n approximately. The higher-order coefficients, which are the amplitudes of the rapidly (space) varying functions, will in fact be determined exactly (in the limit as $n \to \infty$) by the quasi-static field in the neighborhood of the singularity of the iris edge. With this approximate method for determining the A_n in mind, we reconsider Eq. 20. Regarded as a function of the transverse coordinate, Eq. 20 vanishes over the aperture region but has unknown behavior on the iris surface. Since the transverse electric field vanishes on the iris surface, the vector product of Eq. 20, with the transverse electric field at $z = 0$, vanishes everywhere in the waveguide cross section. From Eqs. 14a and 20, therefore, we must have

$$\sum_m \sum_n \frac{A_m A_n}{k_n} \left[\tanh \frac{k_n L}{2} \cos^2 \frac{h_o L}{2} + \coth \frac{k_n L}{2} \sin^2 \frac{h_o L}{2} \right] \cdot (\nabla_T \phi_n \times i_z) \times \nabla_T \phi_m = 0 \qquad (24)$$

over the waveguide cross section. Now since the $\nabla_T \phi_n$ are orthogonal over this region, Eq. 24 can be integrated over the region to obtain

$$\sum_n \frac{A_n^2}{k_n} \left[\tanh \frac{k_n L}{2} \cos^2 \frac{h_o L}{2} + \coth \frac{k_n L}{2} \cos^2 \frac{h_o L}{2} \right] = 0 \qquad (25a)$$

where we assume that the transverse parts of the wave functions have been normalized so that

$$\int_{\substack{\text{waveguide} \\ \text{cross section}}} |\nabla_T \phi_n|^2 \, dS = 1 \qquad (25b)$$

Finally, rewriting Eq. 25a so that the solution for the propagation constant is indicated more explicitly, we obtain

$$\tan^2 \frac{h_o L}{2} = - \frac{\sum_n A_n^2 \dfrac{\tanh (k_n L/2)}{(k_n L/2)}}{\sum_n A_n^2 \dfrac{\coth (k_n L/2)}{(k_n L/2)}}, \quad k_n = \left(p_n^2 - k^2 \right)^{1/2} \qquad (26)$$

Equation 26 is the desired formal result; from here it is only necessary to calculate the A_n from the equivalent static field to complete the relation for a numerical solution.

One notes that Eq. 25a or Eq. 26 can be interpreted to predict the correct result for the limiting cases of both a vanishingly small iris hole and a vanishing iris surface. The fact that the field amplitudes A_n appear as a squared factor suggests that Eq. 26 is capable of interpretation in terms of the energy stored in a period of the structure. Though it is not our intention to do so here, this matter could be pursued further to determine whether or not Eq. 26 is a stationary form.

Now, to complete Eq. 26 for a numerical solution, we calculate the A_n from

$$\overline{E}_T \Big|_{\text{aperture}} = \sum_n A_n \nabla_T \phi_n \tag{27a}$$

$$A_n = \int_{\text{aperture}} \overline{E}_T \cdot \nabla_T \phi_n \, dS \tag{27b}$$

To get down to specific cases, the functions $\nabla_T \phi_n$, their corresponding characteristic numbers p_n, and the calculation of A_n are given for the waveguide geometries in mind.

Case I. Round Waveguide

$$\nabla_T \phi_n = \bar{i}_r \frac{J_1(u_n r/b)}{\pi^{1/2} b \, J(u_n)} \tag{28a}$$

where u_n is the n-th root of $J_o(u_n) = 0$, and $p_n = u_n/b$.

The exact static field in a circular hole of radius a in an infinitely extending transverse plane which intercepts a uniform longitudinal field (see ref. 11, p. 160) is given by

$$\overline{E}_T = \begin{cases} \bar{i}_r \dfrac{r/a}{\left[1 - (r/a)^2\right]^{1/2}} & r < a \\ 0 & r > a \end{cases}$$

Thus, neglecting constant multipliers, we find

$$A_n = \frac{1}{J_1(u_n)} \int_0^a \frac{r/a}{\left[1 - (r/a)^2\right]^{1/2}} J\left(\frac{u_n r}{b}\right) r dr$$

We then make the change in variable, $r = a \sin\theta$, and carry out the integration, using the integral relation (see ref. 13, p. 373)

$$J_{m+n+1}(W) = \frac{W^{n+1}}{2^n \Gamma(n+1)} \int_0^{\pi/2} J_n(W \sin\theta) \sin^{m+1}\theta \cos^{2n+1}\theta \, d\theta$$

where $\mathrm{Re}(n)$ and $\mathrm{Re}(m) > -1$.

The resulting form for A_n is

$$A_n = \left[\frac{1}{(u_n)^{1/2}}\right] \frac{J_{3/2}\left[u_n(a/b)\right]}{J_1(u_n)} \tag{28b}$$

Case II. Infinite Parallel-Plane Waveguide; E_y Odd about the Midplane

$$\nabla_T \phi_n = \bar{i}_y \, 2^{1/2} \sin \frac{(2n+1)\,\pi y}{2b}$$

$$p_n = \frac{(2n+1)\,\pi}{2b}, \quad n = 0, 1, 2, \ldots \tag{29a}$$

The exact static field in the slit of an infinitely extending transverse plane intercepting a uniform longitudinal field (see ref. 11, p. 91) is given by

$$E_T = \begin{cases} \bar{i}_y \dfrac{y/a}{\left[1 - (y/a)^2\right]^{1/2}} & y < a \\ 0 & y > a \end{cases}$$

Thus, again neglecting constant multipliers, we have

$$A_n = \int_0^a \frac{y/a}{\left[1 - (y/a)^2\right]^{1/2}} \sin \frac{(2n+1)\,\pi y}{2b}\, dy$$

The integration is carried out by making the change in variable, $y = a \sin \theta$, and using the integral relation (see ref. 14, p. 150)

$$J_{2n+1}(W) = \frac{2}{\pi} \int_0^{\pi/2} \sin(W \sin\theta) \sin(2n+1)\,\theta \, d\theta$$

The resulting form for A_n is

$$A_n = J_1\left[\frac{(2n+1)\,\pi a}{2b}\right] \tag{29b}$$

Case III. Infinite Parallel-Plane Waveguide; E_y Even about the Midplane

$$\nabla_T \phi_n = \bar{i}_y \, \delta_n \cos \frac{n\pi y}{b}, \quad \delta_n = \begin{cases} 1, & n = 0 \\ 2^{1/2}, & n > 0 \end{cases}$$

$$p_n = \frac{n\pi}{b}, \quad n = 0, 1, 2, \ldots \tag{30a}$$

The exact static field in the slit between two semi-infinite parallel planes with potential

difference between (see ref. 12, p. 106) is

$$\overline{E}_T = \begin{cases} \bar{i}_y \dfrac{1}{\left[1 - (y/a)^2\right]^{1/2}} & y < a \\ \\ 0 & y > a \end{cases}$$

Thus, neglecting constant multipliers, we find

$$A_n = \delta_n \int_0^a \frac{\cos n\pi y/b}{\left[1 - (y/a)^2\right]^{1/2}} \, dy$$

The integration is carried out by making the change in variable, $y = a \cos \theta$, and using the integral relation (see ref. 14, p. 150)

$$J_{2n}(W) = \frac{2}{\pi} \int_0^{\pi/2} \cos(W \sin \theta) \cos 2n\theta \, d\theta$$

The resulting form for A_n is

$$A_n = \delta_n J_o\left(\frac{n\pi a}{b}\right); \quad \delta_n = \begin{cases} 1, & n = 0 \\ \sqrt{2}, & n > 0 \end{cases} \tag{30b}$$

Having calculated the coefficients A_n and indicated the characteristic numbers p_n, we are now in a position to solve numerically for the propagation constant for any of the three cases. In the sums we have to deal with in Eq. 26, only the first few terms are influenced by the frequency; this leaves remainder sums which are functions of the waveguide geometry only. Since the hyperbolic factors in the remainder sums can, for all practical purposes, be equated to unity, the remainder sums each take the form

$$R\left(\frac{a}{b}, \frac{L}{b}\right) = \sum^{\infty} \frac{A_n^2}{(p_n L/2)} \tag{31}$$

The rate of convergence of these sums depends upon the ratio a/b and is especially slow when this ratio is small. Generally speaking, a termwise summation is too tedious to render the calculation useful in practice. Following the technique used in reference 7, section A-7, the author was able to obtain a rapidly converging power series representation of the function R for both of the rectangular waveguide problems. For the range $a/b \leqslant 1/2$, the first two terms of the power series are adequate to describe the function. The series (5) and (6) given in Appendix A apply to Cases II and III, respectively. Using this simplifying technique, the calculation given in Eq. 26 has been carried out for a particular waveguide (Case III), and the results plotted in Fig. 4 from the values

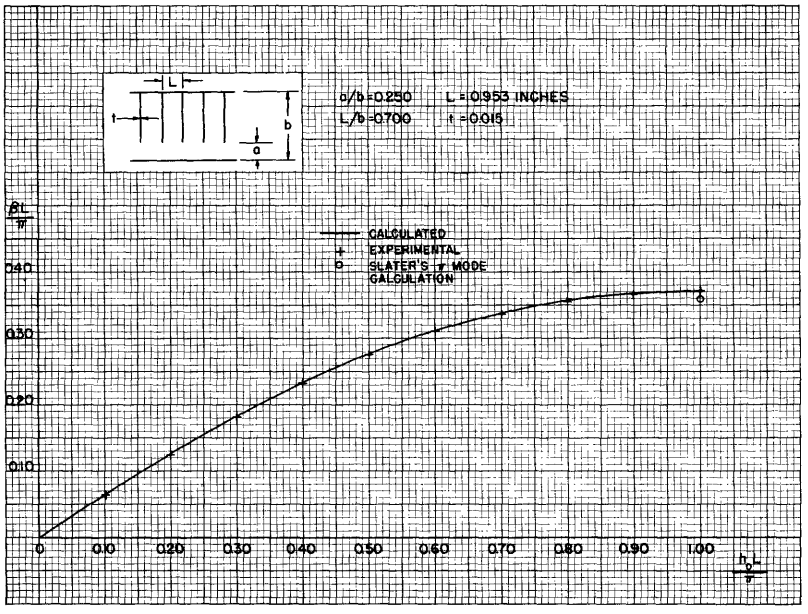

Fig. 4

The propagation characteristic for an iris-loaded rectangular waveguide.

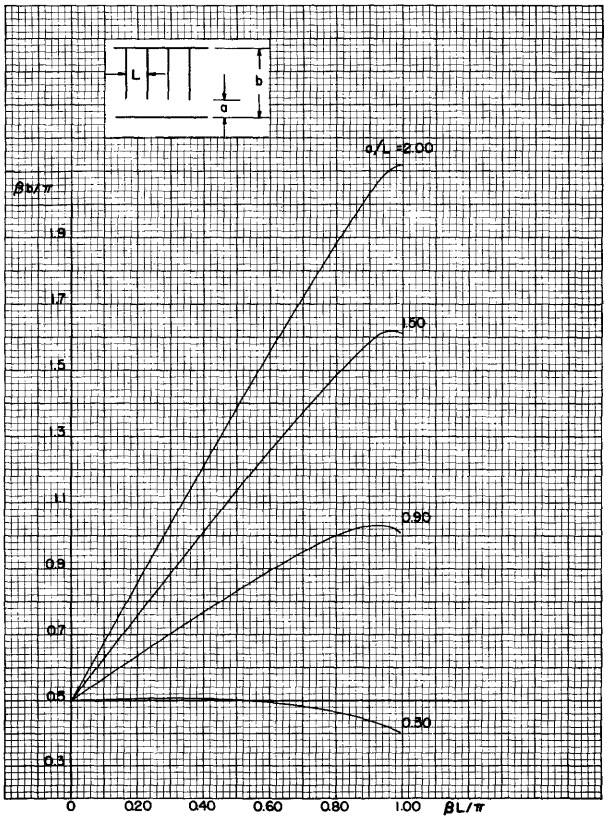

Fig. 5

The π-mode guide wave numbers in an iris-loaded rectangular waveguide.

in Table I(b). Measured results for this case are tabulated in Table I(a) and plotted in Fig. 4 for a comparison.

The frequency at which $h_o L = \pi$ can be calculated directly, using the method of Slater. This calculation proceeds exactly as in reference (2) for the round waveguide, except that the wave functions of the circular cylinder are here replaced by trigonometric functions. The results of this calculation are plotted in Fig. 5 from the values in Table II. The π-mode frequency (or guide wavelength) predicted from this calculation for the particular guide considered in the sample calculation above is indicated in the plot of Fig. 4.

Table I

Table of Values for Curves of Fig. 4

(a) Experimental

$\lambda_c = 14.42$ cm

$h_o L/\pi$	Measured Resonant Wavelength λ_o	$\lambda_g = \frac{\lambda_o}{\left[1 - (\lambda_o/\lambda_c)^2\right]^{1/2}}$	$\frac{\beta L}{\pi} = 2L/\lambda_g$
1.0	9.706 cm	13.05 cm	0.371
0.9	9.758	13.20	0.367
0.8	9.918	13.63	0.355
0.7	10.190	14.38	0.337
0.6	10.600	15.63	0.310
0.5	11.160	17.55	0.276
0.4	11.882	20.87	0.232
0.3	12.704	26.70	0.181
0.2	13.530	39.10	0.124
0.1	14.180	75.80	0.064

(b) Calculated

$\beta L/\pi$	$h_o L/\pi$
0.150	0.242
0.200	0.333
0.250	0.434
0.300	0.562
0.350	0.756
0.365	0.868

The measured results were obtained by observing the resonant frequencies of a ten-section, iris-loaded, rectangular waveguide cavity. The cavity represents Case III of the preceding calculations with a conducting plane placed midway between the broad faces of the guide. The construction of only one half the guide is, of course, a practical simplification. Very thin (1/64 inch) irises were used in order that discrepancies between measured and calculated results could not be attributed, to any appreciable extent, to finite iris thickness.

Table II

Table of Values for Plot of Fig. 5

$\beta L/\pi$	$\beta b/\pi$			
	a/L = 0.30	a/L = 0.90	a/L = 1.50	a/L = 2.00
0.10	0.502	0.568	0.628	0.678
0.30	0.506	0.702	0.883	1.033
0.50	0.502	0.832	1.133	1.383
0.70	0.484	0.951	1.374	1.724
0.90	0.439	1.031	1.583	2.035
0.95	0.421	1.030	1.616	2.095
0.99	0.406	1.011	1.614	2.114

To obtain the π-mode frequencies for values of the parameter a/L other than those tabulated above, the following two equations are solved simultaneously:

(a)
$$C\left[1 - \frac{\tan\beta(b-a)}{\left[(\pi/\beta L)^2 - 1\right]^{1/2}} \coth\left\{\frac{\pi a}{L}\left[1 - \left(\frac{\beta L}{\pi}\right)^2\right]^{1/2}\right\}\right] + 0.689 - 0.104\,\frac{\beta L}{\pi}\tan\beta(b-a) = 0$$

(b)
$$-\frac{C}{3}\left[1 + \frac{\left[4 - (\beta L/\pi)^2\right]^{1/2}}{\left[1 - (\beta L/\pi)^2\right]^{1/2}} \coth\left\{\frac{\pi a}{L}\left[1 - \left(\frac{\beta L}{\pi}\right)^2\right]^{1/2}\right\}\right] + 0.871 + 0.159\left[4 - \left(\frac{\beta L}{\pi}\right)^2\right]^{1/2} = 0$$

where $(a/L) \geq 0.3$.

IV. The Interleaved-Fin Structure as a Slow-Wave Circuit for Traveling Wave Amplifiers

4.1 Introduction

From the discussion in the preceding section, it is apparent that the source-free field solutions for even the simplest type of periodic waveguide are relatively complicated. Moreover, we dealt there with only a small part of the problem for these waveguides: attenuating modes and higher-order free modes were not considered. Now if we introduce an electron stream into such a guide to investigate traveling wave amplification, we must deal in one way or another with a mixture of all possible modes, and the problem becomes impossibly difficult to handle rigorously by the field theory. This is generally true when the interaction circuit is periodic and one finds it necessary to make approximations in treating this type of problem. Though in some cases, periodic boundaries can be approximated by appropriate smooth boundaries, to simplify the problem, the case we will consider is not of this nature.

Pierce has developed a general theory of the thin beam traveling wave tube (ref. 8, chap. VII). This theory is a refinement of a simpler theory developed previously (ref. 8, chap. II). Though the general theory states the problem in a compact form, the solution contains a troublesome parameter (the space-charge parameter Q) which must be evaluated from the field theory; this proves to be a very difficult task when the interaction circuit is periodic. Thus, we shall restrict the problem as follows:

a. Let the total beam current be very small. This restricts the gain constant of the growing wave to small values.

b. Let the stream velocity be very nearly equal to the phase velocity of a given space harmonic in the absence of the beam. This assumption, coupled with assumption (a), results in the phase constant of the growing wave being very nearly equal to that of the unperturbed circuit wave.

With these assumptions, one sees from Pierce's "circuit equation" (ref. 8, p. 242) that the term involving the space charge parameter is negligible. It follows that the simple theory which Pierce proposed is valid and the complexity of the problem is reduced to the extent that amplifiers with periodic circuits can be treated. Although assumption (b) prohibits a direct calculation of the amplifying frequency bandwidth (at constant beam voltage), Pierce indicates a result (ref. 2, p. 18) which can be used to determine the bandwidth approximately.

4.2 Some Results of Pierce's First Theory of Traveling Wave Amplification

As set down in the simple theory, the following quantities are of interest:

a. the circuit impedance Z_c, defined by

$$Z_c = \frac{1}{P_t}\left(\frac{E_{zw}}{h}\right)^2 \tag{32}$$

where E_{zw} is the axial component of the electric field in the beam space of the synchronous circuit wave, h is the propagation constant of the synchronous circuit wave, and P_t is the total axial power flow.

b. the beam impedance Z_b, defined as

$$Z_b = \frac{\text{direct beam voltage}}{\text{direct beam current}} \tag{33}$$

The gain parameter C is in turn defined in terms of the circuit and beam impedances

$$C = \frac{1}{2}\left(\frac{Z_c}{Z_b}\right)^{1/3} \tag{34}$$

Within the limitations of the simple theory, the traveling wave gain in decibels per slow wavelength is 47 times the gain parameter C, and the allowable departure of the phase velocity of the circuit wave from that for maximum gain is

$$\frac{\Delta v_p}{v_p} = \pm C$$

If we now define the circuit dispersion d as

$$d = \frac{dv_p/v_p}{d\omega/\omega} = 1 - \frac{v_p}{v_g} \tag{35}$$

where v_p and v_g are the phase and group velocities, respectively, of the synchronous circuit wave, we may say that the frequency bandwidth for amplification is approximately

$$\frac{\Delta\omega}{\omega} = \frac{2C}{d} \tag{36}$$

We now have a basis for estimating amplifier gain and bandwidth; the circuit properties entering into these considerations are the impedance and dispersion parameters.

4.3 General Properties of the Fields in the Interleaved-Fin Structure

Let us now proceed to the investigation of the interleaved-fin structure, which is shown in Fig. 6. The pair of lateral boundaries of the structure parallel to the y, z plane will be considered as being either of two types: (a) perfectly conducting walls, or (b) boundaries which are open to the outside world.

On the basis of experiment, it was found that the manner in which type (b) boundaries influence the field distribution is adequately described as follows: As long as the propagation constant does not lie in or close to a forbidden region (see subsec. 2.4), one can consider the fields to be totally confined within the structure by magnetic walls at the planes $x = \pm(w/2)$.* This approximation will be used whenever we are concerned with

*A magnetic wall forces the tangential magnetic field to vanish at the wall.

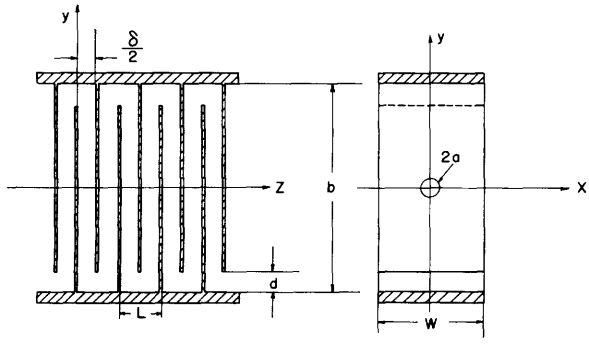

Fig. 6
The interleaved-fin structure.

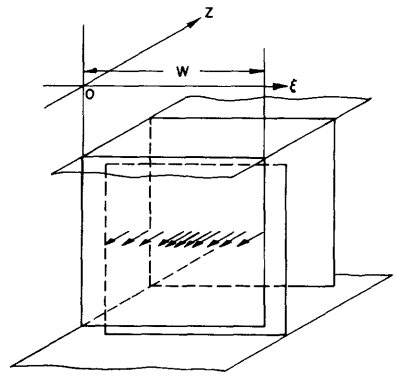

Fig. 7
The characteristic distribution for $E_{z1}^{(1)} = \sin(\pi\xi/w)$.

type (b) boundaries in the following discussion.

The essential nature of the fields in the structure, whether it has type (a) or type (b) boundaries, can be explained from a simple point of view. When the ratios of the structure dimensions are qualitatively like those indicated in Fig. 6 and the beam transmission holes are small ($a \ll w$, $a \ll \lambda_o$), it is natural to regard the structure as a folded waveguide. In this light, possible fields can be constructed from simple traveling waves which run down the structure in the serpentine path between the interleaved fins. For example, in Fig. 7 we show a characteristic distribution for E_z for type (a) boundaries. In the absence of reflection at the bends, this field pattern is a uniform traveling wave in the folded path, propagating as $\exp(-j\beta s)$ (s is the distance measured in the folded path) with E_z reversing direction at each 180° bend. β is related to the frequency and the cutoff wavelength for the characteristic distribution in the usual way.

$$\beta = \left(k^2 - k_c^2\right)^{1/2} \begin{cases} k = \dfrac{\omega}{c} = \dfrac{2\pi}{\lambda_o} \\ k_c = \dfrac{2\pi}{\lambda_c} \end{cases} \tag{37}$$

For this particular distribution or mode, λ_c equals 2w. Higher modes having distributions

$$E_{zm}^{(a)} = \sin\frac{m\pi\xi}{w}, \quad m = 2, 3, 4, \ldots \tag{38a}$$

and cutoff wavelengths

$$\lambda_{cm}^{(a)} = \frac{2w}{m}, \quad m = 2, 3, 4, \ldots \tag{38b}$$

may also propagate.

In the case of type (b) boundaries, the magnetic walls force distributions of

the type

$$E_{zm}^{(b)} = \cos \frac{m\pi\xi}{w}, \quad m = 0, 1, 2, \ldots \tag{39a}$$

with cutoff wavelengths

$$\lambda_{cm}^{(b)} = \frac{2w}{m}, \quad m = 0, 1, 2, \ldots \tag{39b}$$

although, here, m may also take the value zero. In this case the mode is TEM and propagates as exp(-jks). In both cases we exclude propagating characteristic fields which have variations between opposing fin surfaces, for it is always assumed that $L \ll \lambda_o$, a condition which is necessary for good coupling to the electron beam. Thus, although fields having variations between fins are excited at each discontinuity, they damp out rapidly and are confined to a small region in the vicinity of each 180° bend.

4.4 The loaded transmission line model

To define the path s rigorously and, at the same time, consider the effect of reflection at each bend, we shall replace the discontinuity region between uniform line sections by an equivalent transfer network for the propagating wave. Let us anticipate a result and represent the network by a pure shunt susceptance with terminal planes at $y = \pm(b/2)$. Then for the possible propagating fields, the structure is equivalent to the form shown in Fig. 8.* If, under a given set of conditions, the normalized loading susceptance b' vanishes, then the field is a uniform traveling wave in the now defined path s, and the path length over a period of the structure is $\Delta_p s = 2b$. In the more general case the field is not uniform along s, and we must use some results from the theory of lump-loaded transmission lines to pursue the problem further. For the end results we have in mind (relations for the phase velocity and circuit impedance for the space harmonics of the total field), it is necessary to find the phase shift over a period of the line and the power which flows for a given amplitude of electric field in the plane y = 0.

Adopting the convention indicated in Fig. 9 and letting

$$\frac{E_z^n}{E_z^{n-(1/2)}} = e^{-j\alpha}$$

one finds that α is related to the phase shift in the absence of loading βb and the normalized loading susceptance b' through the transcendental relation

$$\cos \alpha = \cos \beta b - \frac{b'}{2} \sin \beta b$$

The phase shift over a period of the line ϕ, which is defined for fields having the same

*The extension of the uniform guide to the planes $y = \pm(b/2)$ should not be confounding. Looking at the equivalent circuit in another way, we could take the terminal planes at $y = \pm(b/2 - d)$; then, insofar as a characteristic field in the uniform guide is concerned, the discontinuity appears as a shunt susceptance viewed through a length of line d on either side.

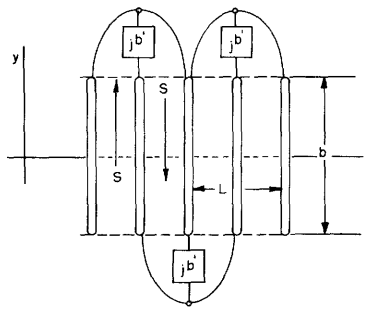

Fig. 8

The equivalent folded waveguide for the propagating wave.

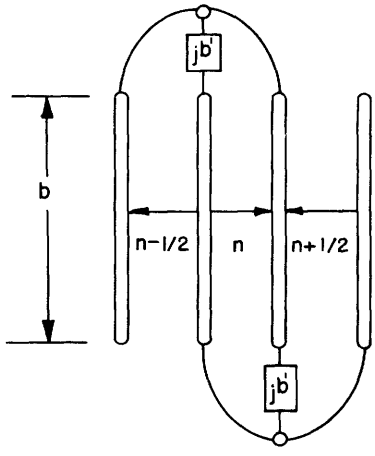

Fig. 9

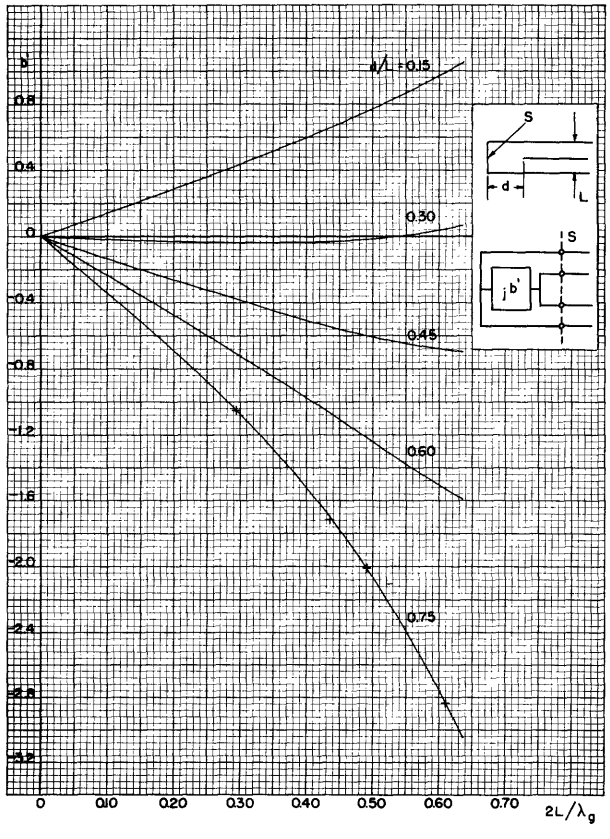

Fig. 10

The normalized susceptance of the 180° bend.

assumed positive direction, is just 2a. Thus

$$\cos\frac{\phi}{2} = \cos\beta b - \frac{b'}{2}\sin\beta b \tag{40}$$

In terms of the z-component of electric field in the plane y = 0, the power flow is given by

$$P = \frac{1}{2Z_{wi}} \iint_{\text{guide cross section}} \left|E_z(x, o, z)\right|^2 dS \tag{41a}$$

where the iterative wave impedance for the plane y = 0, Z_{wi}, is defined by

$$Z_{wi} = \left[\frac{k}{\beta}\left(\frac{\mu}{\epsilon}\right)^{1/2}\right]\left(\tan\frac{\beta b}{2}\cot\frac{\phi}{4}\right) \tag{41b}$$

The loading susceptance b' is implicit in the calculation (Eq. 41b) through the relation indicated by Eq. 40. One notes that in the absence of loading, the factor $\left[\tan(\beta b/2)\cot(\phi/4)\right]$ becomes unity and the iterative wave impedance becomes the familiar uniform wave impedance.

The determination of the equivalent circuit of the 180° bend is a rather lengthy calculation and is deferred to Appendix B. The normalized loading susceptance b' does not depend explicitly upon the type of characteristic field but is a function only of its guide wavelength. One notes from the plotted results in Fig. 10 the rather surprising result that when d/L is adjusted for the ratio 0.3, the loading susceptance is practically zero over a considerable range of guide wavelength.

At this stage the folded waveguide concept has been developed to the extent of its usefulness; it now remains to interpret these results in terms of a set of component waves which run in the z-direction.

4.5 The phase velocities of the space harmonic fields

Recalling from subsection 2.1 the fundamental property of a given mode in a periodic structure, one finds that each vector component of the total field (in particular, we shall be concerned with the component E_z) must obey the periodicity relation

$$E_z(x, y, z) = E_z(x, y, z-L)\exp(-jh_oL) \tag{42a}$$

Hence, it is expressible in the series form

$$E_z(x, y, z) = \sum_{n=-\infty}^{\infty} E_{zn}(x, y)\exp\left[-j\left(h_o + \frac{2\pi m}{L}\right)z\right] \tag{42b}$$

The components $E_{zn}(x, y)$ are the space harmonic amplitudes of the axial electric field in a given mode (corresponding to a given characteristic field in the folded waveguide) and travel along the z-axis with phase velocity

$$\frac{v_{pn}}{c} = \frac{k}{h_o + (2\pi n/L)} = \frac{kL}{h_o L + 2\pi n} \tag{42c}$$

Thus, the problem of determining the phase velocity of any space harmonic at a given frequency is that of finding $h_o L$ at that frequency. $h_o L$ is, of course, the phase shift between the total field quantities at any pair of corresponding points separated by a structure period. By choosing the points to lie on the axis of the structure, where, for all practical purposes, only the dominant wave of the folded guide exists, we can use the equivalent circuit formulation for the dominant wave to deduce that $h_o L$ should be just the phase shift given by Eq. 40.

4.6 Measurement of the propagation characteristic, kL vs $h_o L$, and comparison with theoretical results

To compare the propagation characteristic predicted by Eq. 40 with the measured results, we choose a structure with open boundaries (in this case the experimental results will indicate the validity of the magnetic wall approximation) which has been adjusted for the no-loading condition, $(d/L) = 0.3$. In the absence of loading, Eq. 40 indicates that $h_o L/2 = \beta b$. By covering a sufficiently large frequency range, we can show the presence of a few of the lower modes corresponding to the lower characteristic fields given by Eq. 39. In the case of the lowest mode (for which $m = 0$), β equals k, and we have

$$h_o L = 2kb, \quad m = 0 \tag{43a}$$

For the next higher even mode (our experiment is set up to detect only the even modes), we have

$$h_o L = 2\left[(kb)^2 - (k_c b)^2\right]^{1/2}, \quad k_c = \frac{2\pi}{w}, \quad m = 2 \tag{44a}$$

Since the structure has open boundaries, we will expect forbidden regions of the propagation constant, as indicated in subsection 2.4. For this reason it is convenient to plot the propagation characteristics given in Eqs. 43a and 44a in the $(kL/2\pi, h_o L/2\pi)$ plane and we accordingly rewrite these expressions in the form

$$\frac{kL}{2\pi} = \left(\frac{L}{2b}\right)\frac{h_o L}{2\pi}, \quad m = 0 \tag{43b}$$

$$\frac{kL}{2\pi} = \left(\left[\left(\frac{L}{2b}\right)\left(\frac{h_o L}{2\pi}\right)\right]^2 + \left(\frac{L}{w}\right)^2\right)^{1/2}, \quad m = 2 \tag{44b}$$

To check these results experimentally, the setup sketched in Fig. 11 is used; this makes use of the principle discussed in subsection 2.5. The resonator is five structure periods in length; resonances are thus observed at

$$h_o L/2\pi = 0.1, 0.2, 0.3, \ldots$$

for each mode, provided, of course, that these values do not lie in the forbidden regions. By measuring the frequencies at which these resonances occur, a point-by-point representation of the propagation characteristic is obtained. The results of theory and experiment are compared in Fig. 12. One notes that the theory, which is founded on relatively simple ideas, predicts the propagation constant quite accurately, particularly in the case of the m = 0 mode where the propagation constant does not depend upon the width w. In the case of the second higher mode, the measurements show that the apparent width of the structure is slightly greater than w and varies somewhat with the frequency. This is the type of result one would expect qualitatively. The investigation of the higher modes is, in a sense, academic since a narrow structure propagating in the m = 0 mode will be found most useful in practice. Though experimental results were not obtained for type (a) boundaries, it is felt that the theory should be very accurate in this case. When the boundaries are of type (a), we expect from Eq. 40 propagation characteristics of the type shown in Fig. 13.

One notes from Eq. 42c that the phase velocities of the various space harmonics are readily determined from the propagation characteristic by means of the simple construction shown in Fig. 14. By means of this construction, a basic result is readily established. From the discussion of subsection 2.3, one recalls that the slope of the propagation characteristic $(dk/dh_o) = (1/c)(d\omega/dh_o)$ cannot be negative. One thus sees from Fig. 14 that it is impossible to have a situation in which a space harmonic traveling towards the source ($v_n/c < 0$) has a phase velocity independent of frequency over any small range.

4.7 Space harmonic analysis

Before proceeding to an analysis of the total field into its space harmonic components, we note that the symmetry peculiar to the interleaved-fin structure requires that the total field satisfy the general relation

$$E_z(x, y, z) = -E_z\left[x, -y, z - (L/2)\right] \exp\left(\frac{-jh_o L}{2}\right) \tag{45}$$

This property, when substituted in Eq. 42b for the particular case, y = 0, leads to the result

$$E_{zn}(x, o) = 0 \quad \text{for} \quad n = 0, \pm 2, \pm 4, \ldots \tag{46}$$

That is to say, in the plane y = 0, all the even-order space harmonics (including zero) are absent. In particular, if it is desired to couple an electron beam to the zeroth space harmonic of the m = 0 mode (this wave component has phase velocity substantially independent of frequency), it is necessary to pass the beam along a path off the structure axis. This point is incidental, since we shall be concerned in this report only with the case of coupling at y = 0.

The eventual purpose of a space harmonic analysis is to allow a calculation of the circuit impedance (Eq. 32) for the various space harmonic components. For purposes

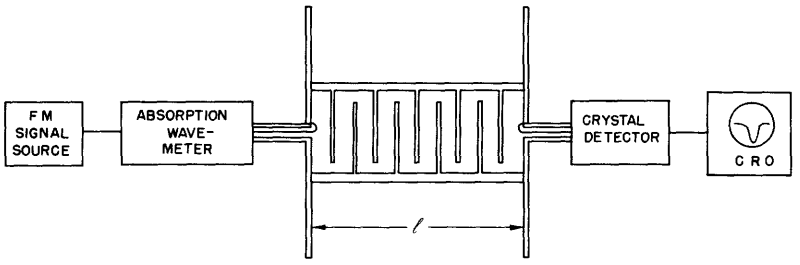

Fig. 11

The experimental setup used to measure the transmission frequencies of the interleaved-fin resonator.

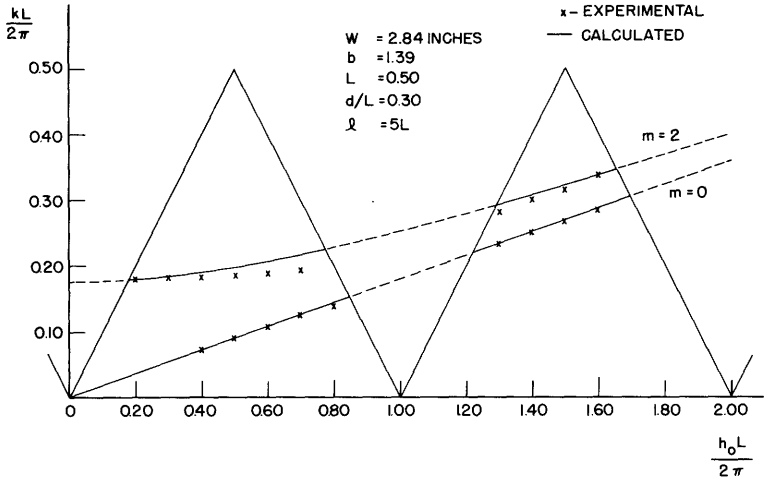

Fig. 12

The propagation characteristic for the first two even transverse variations of the fields in the interleaved-fin structure.

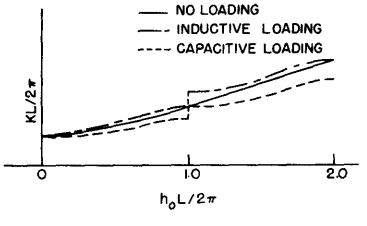

Fig. 13

Propagation characteristics in the guide with type (a) boundaries.

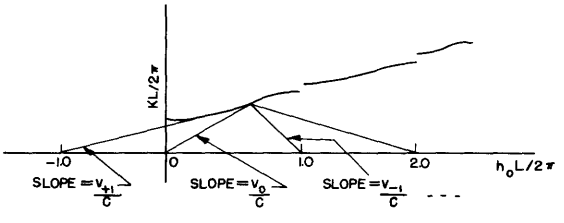

Fig. 14

The construction which determines the space harmonic phase velocities.

of simplicity, it is necessary to assume that the beam to be introduced is very thin; in fact, it is only in this case that the circuit impedance parameter can be defined in the simple manner (Eq. 32). In calculating the circuit fields, we shall accordingly continue to neglect the presence of the beam transmission holes. Calculated on this basis, the impedance parameter for a given space harmonic will not be far wrong, provided the holes are small as compared with the space harmonic wavelength.

Let us suppose that the beam is to be transmitted along the line $x = x_o$, $y = 0$, where x_o is so chosen that the axial electric field has maximum amplitude. Letting the magnitude of E_z between the fins and along this line be E_o, we have in the coordinate system of Fig. 6

$$E_z(x_o, o, z) = \begin{cases} E_o & , \quad 0 < z < \frac{\delta}{2} \\ 0 & , \quad \frac{\delta}{2} < z < \frac{L}{2} \\ -E_o \exp(-jh_o L/2) & , \quad \frac{L}{2} < z < \frac{L+\delta}{2} \\ 0 & , \quad \frac{L+\delta}{2} < z < L \end{cases}$$

Expanding this function in the series

$$E_z(x_o, o, z) = \sum_{n=-\infty}^{\infty} E_{zn}(x_o, o) \exp\left\{-j\left[h_o + (2\pi n/L)\right]z\right\}$$

one finds

$$\left|E_{zn}(x_o, o)\right| = \begin{cases} E_o \dfrac{\sin\left(\frac{\pi}{2}\frac{\delta}{L}\right)\left(\frac{L}{\lambda_{z,n}}\right)}{\left(\frac{\pi}{2}\frac{L}{\lambda_{z,n}}\right)} & , \quad n \text{ odd} \\ 0 & , \quad n \text{ even} \end{cases} \tag{47}$$

where

$$\lambda_{z,n} = \frac{2\pi}{h_o + 2\pi n/L}$$

is the n-th space harmonic wavelength. For the particular case $\delta = L$ (the fin thickness is vanishingly small) the amplitude spectrum is of the form shown in Fig. 15. As the frequency increases, the $h_o L$ increases, and the lines slide to the right as a group within the (sin x/x) envelope. Decreasing the frequency to zero (or the lower cutoff) moves the -1 space harmonic to the point $(L/\lambda_{z,-1}) = -1$, the +1 space harmonic to the point $(L/\lambda_{z,+1}) = +1$, and so forth. Thus, the dominant space harmonic at low frequencies is the -1 space harmonic. More generally, the space harmonic with the longest

wavelength is dominant and remains dominant throughout the range $-1 < (L/\lambda_{z,n}) < +1$.

The impedance parameter given in Eq. 32 also favors the longer wavelength space harmonics through the factor $1/h^2$; we thus form the general conclusion that the circuit couples best to high-voltage electron streams. Using the result of Eq. 47 with that of Eq. 41a to compute the impedance parameter, one obtains the relation

$$Z_{cn,m} = \left\{ a_m \left(\frac{\mu}{\epsilon}\right)^{1/2} \frac{\delta}{w} \frac{k}{\beta_m} \tan \frac{\beta_m b}{2} \cot \frac{h_o L}{4} \right\} \times \left\{ \left(\frac{\sin \frac{\delta}{L} \frac{\pi}{2} \frac{L}{\lambda_{z,n}}}{\frac{\delta}{L} \frac{\pi}{2} \frac{L}{\lambda_{z,n}}} \right) \left(\frac{1}{\frac{L}{\lambda_{z,n}}} \right) \right\}^2 \qquad (48)$$

where the subscript m denotes the mode of propagation and the subscript n denotes a particular space harmonic of this mode. The quantity a_m distinguishes between the characteristic fields with sinusoidal x variation and the one with no variation,

$$a_m = \begin{cases} 1, & m = 0 \\ 2, & m > 0 \end{cases}$$

The factor $\tan (\beta_m b/2) \cot (h_o L/4)$ arises from the periodic loading in the folded guide and is significant in the case of closed boundaries when the phase shift between discontinuities, $h_o L/2$, is an integer multiple of π. If the structure has open boundaries, these critical values are not allowed; otherwise, this factor becomes either zero or infinite according to the patterns shown in Fig. 16(a) and (b). A pole due to the factor $\tan (\beta_m b/2) \cot (h_o L/4)$ may not be a pole of the impedance parameter for all space harmonics, since at the critical values $h_o L/2\pi = q$, an odd integer, one notes from Fig. 15 that only a single space harmonic is present, the -q-th. The notation, -1, in Fig. 16(a) and (b) serves to indicate a pole for the -1 space harmonic only (implying a zero for all others), and an extended plot would show a similar notation at $h_o L/2\pi = 3, 5$, and so forth. By adding to these plots a pole at $h_o L/2\pi = 0$ which results from the low-frequency cutoff, all critical values of the circuit impedance relation (see Eq. 48) are shown.

4.8 Coupling to the -1 space harmonic of the m = 0 mode

In the foregoing discussion, we attempted to show the general nature of the impedance parameter and the phase velocity of the space harmonic fields; we have derived relations which will determine these quantities for any particular geometry, frequency, and structure mode. We shall not try to anticipate all the possible applications of the structure as an interaction circuit nor specialize the results to these applications. However, the m = 0 mode of the open-boundary structure is worthy of special consideration since, for propagation in this mode, the structure width can be quite small. It is thus generally possible to obtain relatively large values of the coupling impedance without operating in the region of an impedance pole, where the impedance is large only over a narrow frequency band.

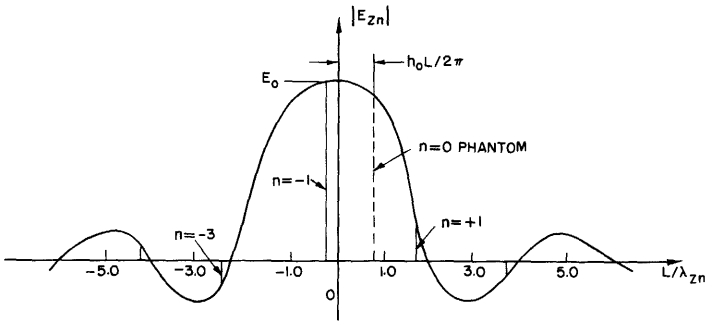

Fig. 15

Spectrum of the space harmonic amplitudes.

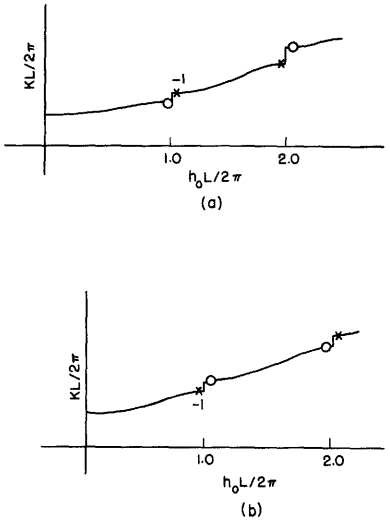

Fig. 16

Zeros and poles of the impedance parameter due to the factor $\left[\tan(\beta_m b/2)\cot(h_o L/4)\right]$ for the case (a) of capacitive loading $\left[(d/L) < 0.3\right]$ and case (b) of inductive loading $\left[(d/L) > 0.3\right]$.

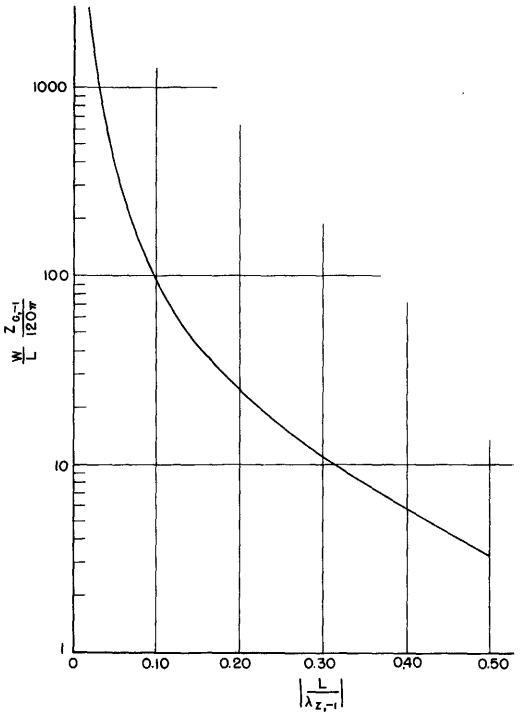

Fig. 17

Coupling impedance of the -1 space harmonic.

All other things being equal, large impedances result when the spacing between fins is a small fraction of the coupled-wave wavelength. When the spacing meets this requirement, the loading susceptance of the 180° bend is very small, as we note from Fig. 10. In this case the following simplifications result: (a) The periodic loading factor, $\tan(\beta_m b/2)\cot(h_o L/4)$ in the impedance expression is replaced by unity. (b) The propagation characteristic is computed on the basis of no loading, $h_o L = 2kb$.

At a given frequency, the phase shift over a period of the structure can be adjusted (by adjusting the dimension b) to make any particular space harmonic dominant (consult Fig. 15). Adjusting for dominance of the -1 space harmonic results in the smallest b-dimension and, assuming this to be desirable, we shall consider the case of coupling to the -1 space harmonic field.

Presumably, for a tube design, the electron stream velocity and the free-space wavelength are given quantities. This immediately determines $\lambda_{z,-1}$, and the coupling impedance follows from the ratio $(L/\lambda_{z,-1})$ through the relation indicated in Eq. 48. This relation is plotted in Fig. 17 for the case of vanishing fin thickness ($\delta/L = 1$). The b-dimension necessary to give the required wave velocity is given by

$$\frac{2b}{\lambda_o} = \frac{L}{\lambda_{z,-1}} + 1$$

(Note that the quantity $\lambda_{z,-1}$ can have either a plus or a minus sign according to whether the -1 space harmonic is a forward or a backward wave.) If the frequency is now changed from the design frequency and the stream velocity is held constant, the cold phase velocity differs from the electron velocity and the amplifier gain drops. The frequency bandwidth for amplification is given approximately by Eq. 36, in which we substitute for the dispersion

$$d = \frac{\lambda_{z,-1}}{L}$$

Appendix A

Power Series Expansions of some Schlömilch (and Associated) Series

1) $$\sum_{n=1}^{\infty} \frac{J_o(nx)}{n} \frac{\sin nx}{nx} = \ln \frac{2}{x} + \frac{5x^2}{144} + \frac{7x^4}{12,800} + \ldots \qquad 0 < x < \pi$$

2) $$\sum_{n=1}^{\infty} \frac{J_o(nx)}{n} \cos nx = \ln \frac{2}{x} + \frac{3x^2}{48} + \frac{35}{32} \frac{x^4}{720} + \ldots \qquad 0 < x < \pi$$

3)* $$\sum_{n=1}^{\infty} \frac{J_o(nx)}{n} = \ln \frac{2}{x} + \frac{x^2}{48} + \frac{x^4}{7680} + \ldots \qquad 0 < x < \pi/2$$

4) $$\sum_{q=1,3,5}^{\infty} \frac{J_o(qx)}{q} = \frac{1}{2} \ln \frac{2}{x} - \frac{x^2}{48} - \frac{21x^4}{23,040} - \ldots \qquad 0 < z < \pi$$

5) $$\sum_{q=1,3,5}^{\infty} \frac{J_1^2(qx)}{q} = \frac{1}{4} + \frac{x^2}{48} + \frac{21}{20} \frac{x^4}{288} + \ldots \qquad 0 < x < \pi/2$$

6)* $$\sum_{n=1}^{\infty} \frac{J_o^2(nx)}{n} = \ln \frac{2}{x} + \frac{x^2}{24} + \frac{x^4}{1280} + \ldots \qquad 0 < x < \pi/2$$

7)* $$\sum_{n=1}^{\infty} \frac{J_o(nx)}{n^2} = \frac{\pi^2}{6} - x + \frac{x^2}{8}$$

*These sums were computed in reference (7).

Appendix B

Equivalent Circuit of the 180° Bend

As a result of treating the interleaved-fin structure as a folded waveguide, we are confronted with the problem of determining the equivalent circuit for a 180° bend in the waveguide. There are two types of waveguide to consider; these are indicated in Figs. B-1(a) and B-1(b) and correspond to the cases of open and closed lateral boundaries, respectively. In practice, the dimension L/2 will always be a very small fraction of a free-space wavelength; as a result, only waves from the class of $H_{m,o}$ waves can propagate (m refers to x-variations, o to y-variations). Now if, in either guide, a propagating $H_{m,o}$ wave is incident upon the discontinuity, only waves with variations of the m type are excited. From this fact it is not difficult to show that the solution for any of the admissible m-variations of the incident wave can be obtained from the solution for a particular value of m, say m = j, by substituting λ_{gm} for λ_{gj}. The simplest problem to solve directly is that for j = 0, or the case of an incident TEM wave. This is the problem we shall deal with in detail.

The principles of microwave circuits lead us to the boundary-value problem which must be solved to determine the equivalent circuit parameters. We first assume that the effect of the discontinuity on the propagating wave can be represented by a T-network joining the uniform sections of waveguide. The proof of the existence of such a network (which implies the reciprocity relation) follows from the fact that the system is completely closed. The solution can be simplified somewhat by making use of apparent symmetry properties (see Fig. B-2). If the terminal planes for the equivalent network T_1 and T_2 are symmetrically located with respect to the discontinuity, the network is symmetric, and $Z_{11} = Z_{22}$. We must then in some convenient way solve for the remaining two quantities Z_{12} and Z_{11} (or Z_{22}). Figures B-2(a) and B-2(b) illustrate the application of Bartlett's bisection theorem for symmetric networks in reducing the problem to the solution for two driving-point impedances. With dominant waves incident upon the discontinuity as in Fig. B-2(a), each wave sees $Z_{11} - Z_{12}$ at its terminal plane. We see that in this case tangential electric fields cancel in the plane of symmetry and a conducting plane can be placed here (indicated by the heavy line). A convenient choice for the location of the terminal planes is thus in the surface S; then we have $Z_{11} - Z_{12} = 0$, and the equivalent network is a pure shunt impedance. With the excitation as in Fig. B-2(b), the dominant wave in each guide sees $Z_{11} + Z_{12} = 2Z_{12}$ at its terminal plane. In this case, the tangential magnetic fields cancel in the plane of symmetry, and a magnetic wall can be placed here (indicated by the dashed line). To determine the shunt impedance of the discontinuity, we thus solve the boundary value problem in either half of the folded guide, replacing the aperture by a magnetic wall (Fig. B-3). The impedance seen by the dominant wave at z = 0 (or any integer number of half-wavelengths back from this plane) is just twice the shunt impedance for the equivalent

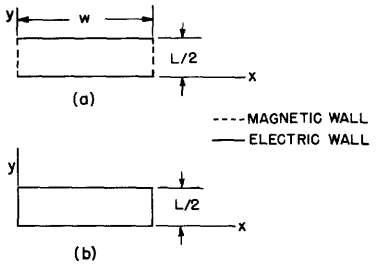

Fig. B-1

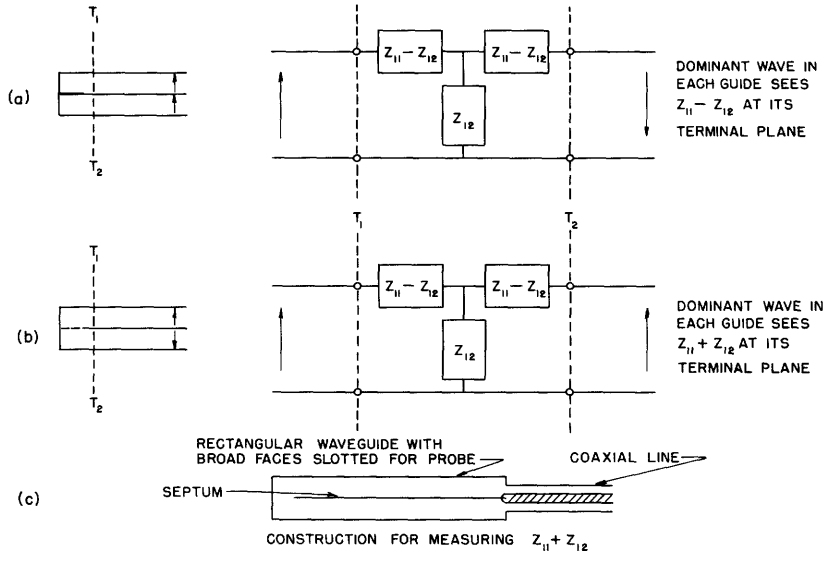

Fig. B-2

The application of Bartlett's bisection theorem to the equivalent network for the 180° bend.

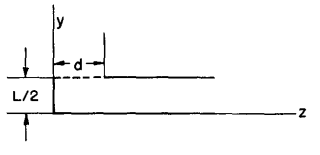

Fig. B-3

The half-guide, in which the aperture has been replaced by a magnetic wall.

network representation of the 180° bend.

We now turn to the solution of Maxwell's equations in the geometry of Fig. B-3. A dominant wave incident upon the discontinuity will produce a reflected dominant wave, plus a local field distribution in the vicinity of the discontinuity. Since the exciting dominant wave fields do not vary with coordinate x, and the structure is uniform in the x-direction, none of the field quantities will vary with coordinate x. This being the case, no current is required to flow in the x-direction, and we can set $H_z = 0$. Now, the Maxwell equations, with $\partial/\partial x = 0$ and $H_z = 0$, reduce to the following form

$$\left[\nabla_{yz}^2 + k^2\right] H_x = 0 \tag{B-1a}$$

$$-j\omega\epsilon\, E_z = \frac{\partial H_x}{\partial y} \tag{B-2b}$$

$$j\omega\epsilon\, E_y = \frac{\partial H_x}{\partial z} \tag{B-1c}$$

The proper general solutions to these equations must be chosen for the two regions, $0 \leqslant z \leqslant d$, $z \geqslant d$, and the transverse electric and magnetic fields matched across the interface, $z = d$. This procedure leads to the exact solution of the problem, all fields being determined to within an arbitrary constant factor. The ratio of the reflected to incident dominant wave amplitudes is uniquely determined, and from this ratio the impedance Z_{12} follows. The boundary conditions which must be satisfied in each region are that the normal derivative of tangential H must vanish at a conducting wall, and that tangential H must itself vanish at the magnetic wall. As can be readily verified, the appropriate solutions to the Eqs. B-1a, b, and c are

$0 \leqslant z < d$

$$H_x = j\omega\epsilon \sum_q A_q \cos p_q y \cosh k_q z \tag{B-2a}$$

$$E_y = \sum_q A_q k_q \cos p_q y \sinh k_q z \tag{B-2b}$$

where $k_q^2 = p_q^2 - k^2$, $p_q = (q\pi/L)$, and $k = (\omega/c)$ $(q = 1, 3, 5, \ldots)$

$z > d$

$$H_x = j\omega\epsilon \left[B_o \exp(-jkz) - C_o \exp(jkz) + \sum_n B_n \cos p_n y \exp(-k_n z)\right] \tag{B-3a}$$

$$E_y = -jk\left[B_o \exp(-jkz) + C_o \exp(jkz)\right] - \sum_n B_n k_n \cos p_n y \exp(-k_n z) \tag{B-3b}$$

where $k_n^2 = p_n^2 - k^2$, $p_n = (2n\pi/L)$ $(n = 1, 2, 3, \ldots)$. Matching total H_x and E_y at $z = d$ gives

$$\sum_q A_q \cosh k_q d \cos p_q y = B_o \exp(-jkd)\left[1 - \Gamma(d)\right] + \sum_n B_n \exp(-k_n d) \cos p_n y \qquad \text{(B-4a)}$$

$$\sum_q A_q k_q \sinh k_q d \cos p_q y = -jkB_o \exp(-jkd)\left[1 + \Gamma(d)\right] - \sum_n B_n k_n \exp(-k_n d) \cos p_n y \qquad \text{(B-4b)}$$

where $\Gamma(d) = (C_o/B_o)\, e^{j2kd}$ is the reflection coefficient for the dominant wave at $z = d$. We must now expand the factors $\cos p_q y$ in terms of the $\cos p_n y$ so that we can equate corresponding coefficients of the functions, $\cos p_n y$, which are orthogonal over the interval $(0, L/2)$. From straightforward Fourier analysis, there follows,

$$\cos p_q y = a_o + \sum_{n=1}^{\infty} a_n \cos p_n y \qquad \text{(B-5a)}$$

$$a_o = \frac{2}{q\pi}(-1)^{(q-1)/2} \qquad \text{(B-5b)}$$

$$a_n = \frac{q}{\pi} \frac{1}{\left(\frac{q}{2}\right)^2 - n^2} (-1)^{(2n+q-1)/2} \qquad \text{(B-5c)}$$

Substituting these results in (B-4a, b) and equating corresponding coefficients of $\cos p_n y$, we obtain

$$B_o \exp(-jkd)\left[1 - \Gamma(d)\right] = \sum_q \frac{2}{q\pi}(-1)^{(q-1)/2} A_q \cosh k_q d \qquad \text{(B-6a)}$$

$$B_n \exp(-k_n d) = \sum_q \frac{q}{\pi} \frac{1}{\left(\frac{q}{2}\right)^2 - n^2} (-1)^{(2n+q-1)/2} \times A_q \cosh k_q d, \quad n = 1, 2, 3, \ldots \qquad \text{(B-6b)}$$

$$jkB_o \exp(-jkd)\left[1 + \Gamma(d)\right] = -\sum_q \frac{2}{q\pi}(-1)^{(q-1)/2} A_q k_q \sinh k_q d \qquad \text{(B-6c)}$$

$$k_n B_n \exp(-k_n d) = \sum_q \frac{q}{\pi} \frac{1}{\left(\frac{q}{2}\right)^2 - n^2} (-1)^{(2n+q-1)/2}$$

$$A_q k_q \sinh k_q d, \quad n = 1, 2, 3, \ldots \qquad \text{(B-6d)}$$

Dividing (c) by (a), (d) by (b), we get an infinite set of simultaneous homogeneous equations for the coefficients A_q:

$$\sum_q \left\{ A_q k_q \sinh k_q d \frac{q}{\left(\frac{q}{2}\right)^2 - n^2} (-1)^{(q-1)/2} \right\}$$

$$\left\{ 1 + \frac{k_n}{k_q} \coth k_q d \right\} = 0, \quad n = 0, 1, 2, \ldots \qquad \text{(B-7)}$$

where, in the n = 0 equation, the quantity

$$jk \frac{1 + \Gamma(d)}{1 - \Gamma(d)} = -jk \left(\frac{Z}{Z_o}\right)'$$

is substituted for jk_o. The normalized impedance $(Z/Z_o)'$ is the impedance seen by the dominant wave in the half-guide at z = d. Once we have solved for this quantity, we must find the corresponding value at z = 0 and divide this by two to obtain Z_{12}.

The equations (Eq. B-7) have nontrivial solutions for the A_q only if the determinant of the coefficients vanishes. Setting the determinant equal to zero furnishes the exact solution for $(Z/Z_o)'$ in terms of the frequency and waveguide dimensions, but, of course, this cannot be carried out in practice and we must look for a method to solve these equations approximately. A method used by Slater (2) solves these equations very accurately; the form of the resulting approximate relation is well suited to a numerical solution.

It is noted from Eq. B-2b that the $A_q k_q \sinh k_q d$ in Eq. B-7 are the Fourier coefficients of the expansion of E_y at z = d in the cosine functions, $\cos(q\pi y/L)$. The equivalent static field in the vicinity of the singularity at z = d will determine the higher Fourier coefficients very accurately. For an approximate solution we will use the static field to determine all but the first (q=1) coefficient. This coefficient can be left open and eliminated between the n = 0 equation and any other equation in the set (Eq. B-7). Now, the equivalent static field becomes infinite inversely as the square root of the distance from the singularity; on the conducting wall at z = d, y = 0, the normal derivative of normal electric field must vanish. The appropriate form for E_y is thus

$$E_y(d) = \frac{1}{\left[1 - (2y/L)^2\right]^{1/2}} \qquad \text{(B-8)}$$

Expanding Eq. B-8 in the cosine functions, $\cos(q\pi y/L)$, we find that the coefficients are given by

$$a_q = A_q k_q \sinh k_q d = J_o\left(\frac{q\pi}{2}\right)$$

Since we do not intend to use the a_q's thus determined for q = 1, the asymptotic form for $J_o(q\pi/2)$

$$J_o\left(\frac{q\pi}{2}\right) \sim \frac{1}{q^{1/2}} (-1)^{(q-1)/2}$$

can be substituted for a_q. In addition, for $q \geq 3$, k_q can be replaced by $(q\pi/L)$, and the factor $\coth k_q d$ can be replaced by unity (to within one percent, provided $d/L > 0.30$). Using these approximations, together with the numerical values of the sums tabulated for m = 0, 2, 4 in reference (2), p. 11, the first three equations of the set (Eq. B-7) take the approximate form

n = 0

$$C\left[1 + \frac{(kL/\pi)\,X}{\left[1 - (kL/\pi)^2\right]^{1/2}} \coth \frac{\pi d}{L}\left[1 - \left(\frac{kL}{\pi}\right)^2\right]^{1/2}\right] + 0.689 + 0.104\left(\frac{kL}{\pi}\right) X = 0$$

n = 1

$$C\left[1 + \frac{\left[4 - (kL/\pi)^2\right]^{1/2}}{\left[1 - (kL/\pi)^2\right]^{1/2}} \coth \frac{\pi d}{L}\left[1 - \left(\frac{kL}{\pi}\right)^2\right]^{1/2}\right] - 3.58 = 0$$

n = 2

$$C\left[1 + \frac{4}{\left[1 - (kL/\pi)^2\right]^{1/2}} \coth \frac{\pi d}{L}\left[1 - (kL/\pi)^2\right]^{1/2}\right] - 6.50 = 0$$

where $jX = (Z/Z_o)'$ and C is proportional to the first Fourier coefficient of the expansion of $E_y(d)$. To solve these equations for a given geometry and frequency, C is determined from either the n = 1 or n = 2 equation and substituted in the n = 0 equation to compute X. In terms of the quantity X we know, from straightforward transmission line relations, that the normalized susceptance at z = 0 for the equivalent circuit representation in the folded guide is

$$b' = -2 \cot(\tan^{-1} X - kd)$$

Using these relations, we have calculated and tabulated the normalized susceptances in Table BI. (Unfortunately, the susceptance was computed for values of kL/2 rather than kL/π.)

It was found that the values of C calculated from the n = 1 and n = 2 equations agreed quite well, indicating that the approximate method of solution should be very accurate.

To check the results of the calculation experimentally, the measuring scheme shown

Table BI

Values of the Normalized Shunt Susceptance of the 180° Bend

kL/2	d/L				
	0.15	0.30	0.45	0.60	0.75
0.2	0.180	-0.020	-0.169	-0.301	-0.429
0.4	0.368	-0.035	-0.333	-0.608	-0.891
0.6	0.568	-0.034	-0.488	-0.930	-1.434
0.8	0.789	-0.008	-0.621	-1.271	-2.127
1.0	1.056	+0.070	-0.702	-1.595	-3.044

in Fig. B-1(c) was used. In this construction, the dominant wave in each guide sees, at the short-circuiting end plane, a susceptance which is just one-half the susceptance for the equivalent circuit of the 180° bend. If the measured distance from the end plane to the point of minimum field strength in the guide is ℓ, the susceptance for the equivalent circuit is just

$$b' = 2 \cot \frac{2\pi\ell}{\lambda_g}$$

To check the symmetry of construction, both broad faces of the waveguide were slotted, and the minimum position measured in each half-guide. The results of the measurements are tabulated in Table BII and plotted with the calculated results in Fig. 9.

Table BII

Table of Measured Results. The Waveguide Construction of Fig. B1(c) Was Used; d/L = 0.75.

λ_g	ℓ_1	ℓ_2	$2L/\lambda_g$	b'
23.15 cm	2.985 in.	2.980 in.	0.294	-1.05
15.65	5.320	5.320	0.435	-1.72
13.84	4.800	4.800	0.491	-2.01
11.14	3.960	3.960	0.610	-2.82

A standard S-band waveguide with a 1/32-inch-thick septum was used for the measurement.

Acknowledgment

The author would like to thank Mr. L. D. Smullin, supervisor of the thesis on which this report is based, and Professors L. J. Chu and R. B. Adler for helpful discussions concerning some aspects of the material that has been presented.

References

1. J. C. Slater: The Design of Linear Accelerators, Technical Report No. 47, Research Laboratory of Electronics, M.I.T., Sept. 1947
2. J. C. Slater: Electromagnetic Waves in Iris-Loaded Waveguides, Technical Report No. 48, Research Laboratory of Electronics, M.I.T., Sept. 1947
3. W. Walkinshaw: Theory of Circular Corrugated Waveguide for Linear Accelerator Telecommunication Research Establishment, Technical Note No. 5301, Aug. 1946
4. E. L. Chu, W. W. Hansen: The Theory of Disc-Loaded Wave Guides, J. Appl. Phys. 18, 996-1008, 1947
5. L. Brillouin: Wave Guides for Slow Waves, J. Appl. Phys. 19, 1023-41, 1948
6. R. B. Adler: Properties of Guided Waves on Inhomogeneous Cylindrical Structures, Technical Report No. 102, Research Laboratory of Electronics, M.I.T., May 1949
7. S. Sensiper: Electromagnetic Wave Propagation on Helical Conductors, Technical Report No. 194, Research Laboratory of Electronics, M.I.T., May 1951
8. J. R. Pierce: Traveling-Wave Tubes, Van Nostrand, New York, 1950
9. L. J. Chu, D. J. Jackson: Field Theory of Traveling-Wave Tubes, Technical Report No. 38, Research Laboratory of Electronics, M.I.T., April 1947
10. S. A. Schelkunoff: Electromagnetic Waves, Van Nostrand, New York, 1943
11. W. R. Smythe: Static and Dynamic Electricity, McGraw-Hill, New York, 1939
12. S. Ramo, J. R. Whinnery: Fields and Waves in Modern Radio, John Wiley, New York, 1949
13. G. N. Watson: A Treatise on the Theory of Bessel Functions, Second Edition, MacMillan, New York, 1948
14. E. Jahnke, F. Emde: Tables of Functions, Dover Publications, New York, 1945
15. F. B. Hildebrand: Notes for course, Methods of Applied Mathematics, Department of Mathematics, M.I.T., Sept. 1950
16. N. Marcuvitz: Waveguide Handbook, Radiation Laboratory Series, Vol. 10, McGraw-Hill, New York, 1951